Evaluation of the compositional changes during flooding of reactive fluids using scanning electron microscopy, nano-secondary ion mass spectrometry, x-ray diffraction, and whole-rock geochemistry

Udo Zimmermann, Merete Vadla Madland, Anders Nermoen, Tania Hildebrand-Habel, Silvana A. R. Bertolino, Aksel Hiorth, Reidar I. Korsnes, Jean-Nicolas Audinot, and Patrick Grysan

ABSTRACT

Outcrop chalk of late Campanian age (Gulpen Formation) from Liège (Belgium) was flooded with $MgCl_2$ in a triaxial cell for 516 days under reservoir conditions to understand how the non-equilibrium nature of the fluids altered the chalks. The study is motivated by enhanced oil recovery (EOR) processes because dissolution and precipitation change the way in which oils are trapped in chalk reservoirs. Relative to initial composition, the first centimeter of the flooded chalk sample shows an increase in MgO by approximately 100, from a weight percent of 0.33% to 33.03% and a corresponding depletion of CaO by more than 70% from 52.22 to 14.43 wt.%. Except for Sr, other major or trace elements do not show a significant change in concentration. Magnesite was identified as the major newly grown mineral phase. At the same time, porosity was reduced by approximately 20%. The amount of Cl^- in the effluent brine remained unchanged, whereas Mg^{2+} was depleted and Ca^{2+} enriched. The loss of Ca^{2+} and gain in Mg^{2+} are attributed to precipitation of new minerals and leaching the tested core by approximately 20%, respectively. Dramatic mineralogical and geochemical changes are observed with scanning electron microscopy–energy-dispersive x-ray spectroscopy, nano secondary ion mass spectrometry, x-ray diffraction, and whole-rock geochemistry techniques. The understanding of how fluids interact with rocks is important to, for example, EOR, because textural changes in the pore space affect how water will imbibe and expel oil from the rock. The mechanisms of dissolution and mineralization of fine-grained chalk can be described and quantified and, when understood, offer numerous possibilities in the engineering of carbonate reservoirs.

INTRODUCTION

The use of fluid injection for improved or enhanced oil recovery (EOR) is a commonly studied subject (e.g., Thomas et al., 1987; Hermansen et al., 2000; Strand et a l., 2007 and references cited therein), and results have been used in the production of hydrocarbons (Hermansen et al., 2000). Laboratory results from the last decades have demonstrated that lowering the salinity of the injection water increases the recovery from sandstones. This has led to studies to investigate the possibility of applying this mechanism on field scale and was followed by several field tests and now a full field injection of low salinity water flooding, the BP Clair Ridge project, has been initiated (BP, 2014). In chalk, the concentration of divalent ions, and in particular magnesium, is an important factor. Several studies have been performed to find the composition of the optimal injection fluid for chalk (Strand et al.,2003; Austad and Standnes, 2003; Madland et al., 2006, 2008; Zangiabadi et al., 2009). The cost of changing injection fluid versus the additional recovery must be addressed for each field specifically, and it is not the scope of this work. However, if the additional recovery is large enough, any type of fluid chemistry could be injected. Previous studies have shown that different ions, for example, Ca^{2+}, Mg^{2+}, SO^{2-}_4 in the injected brine have an impact on both the mechanical stability of chalk rock, and oil recovery from carbonate fields (Strand et al., 2003; Austad and Standnes, 2003; Heggheim et al., 2005; Korsnes et al., 2006, 2008a, b; Madlandet al., 2006, 2008; Zangiabadi et al., 2009). The published research so far, however, emphasizes the complexity of the systems tested. When injecting

seawater, several mechanisms (precipitation, dissolution, ion exchange, adsorption, and desorption) can be active at the same time, and these mechanisms translate to a larger scale in a completely different manner. Therefore, a need to simplify the system has been identified and each ion of importance has been studied individually. In this paper, we focused on the presence of magnesium and used $MgCl_2$ brine for the long-term flow-through experiment (Figure 1).The compaction of a chalk reservoir is experienced at Ekofisk, North Sea. Here, the compaction is not only a result of the increased effective stresses linked to pore pressure depletion during oil recovery. In regions of the reservoirs that have been exposed to seawater injection, enhanced compaction and corresponding seabed subsidence is seen despite regaining pore pressure (e.g., Nagel, 2001; Doornhof et al., 2007). As such, there is an important and substantial chemical component to the observed compaction. It is well known that dissolution will be greater near the injector; however, because of cold temperature fronts, the dissolution front will propagate a distance into the reservoir. How far into the reservoir has to be evaluated in each case and depends on reservoir flow paths, chemical rate constants, and the temperature profile. To use the laboratory results for decision-making processes in reservoir engineering, a correct up-scaling to the reservoir scale is crucially needed. A robust model of the rock-fluid interactions at reservoir scale requires a fundamental understanding of the underlying mechanisms that take place when fluids are injected through reactive rocks in controlled environments; thus, observations from long-term experiments are required. Growth of new mineral phases during the experiments was observed in short-term tests (Madland et al., 2011), but the present core scale experiment is novel with regard to its duration under reservoir temperature (130°C) and values of effective stresses (12.6 MPa). We present here the first long-term test (516 days) on chalk with the injection of $MgCl_2$ under reservoir conditions, although several long-term experiments have been reported before (Hellmann et al., 2002). We will address in detail the chemical changes of the effluent fluid and the corresponding changes to the mineralogy of the flooded sample. Our results show that the degree of chemical alteration is nonuniform throughout the sample, in addition, we provide the outcome of a numerical modeling experiment where rock-fluid interactions and the flow dynamics are incorporated. During long-term injection of $MgCl_2$, we induced extensive precipitation of secondary minerals, which fundamentally changed the chalk rock properties.

GEOLOGIC BACKGROUND

The Liège chalk, like several other Cretaceous outcrop chalk exposures, has been used as analogs material in the study of the mechano-chemical processes during rock-fluid interactions at elevated stresses and temperatures in reservoir chalks (e.g. Hjuler, 2007; Strand et al., 2007). It is found that the same physical and chemical processes are observed in the easily accessible outcrop chalks as those experiments that are performed with reservoir materials (Hiorth et al., 2010). As such, the basic principles in physics and chemistry observed in the outcrop material can be transferred to reservoir rocks with some degree of certainty. However, to select the correct outcrop chalk equivalent to a specific reservoir is a matter of debate (Hjuler, 2007). More than 40 yr of systematic research on chalk mineralogical and geochemical composition has been carried out (e.g., Scholle, 1974, 1977; Hancock, 1975; Fabricius, 2007). Until now, progress has been hampered by the small grain size of the chalk and the too-coarse spatial resolution of the observation techniques. Recently developed analytical techniques that can investigate the composition of nano-sized particles, ultra-high resolution electron microscopy, and high-resolution geochemical methods require little sample material and open new possibilities in the understanding of chalk. In this study, we used chalk from Liège, suggested as the best match for the reservoir successions in the North Sea (Hjuler and Fabricius, 2009). The sampled chalk at Liège belongs to the Campanian to late early Maastrichtian Gulpen Formation, which has been deposited from the Campanian until the late early Maastrichtian (Molenaar and Zijlstra, 1997). The samples here originate from the basal succession, the ZevenWegen Member (Robaszynski et al., 2001) with an age of 75.5–78.0 Ma (belemnite zone Belemnitella mucronata after Slimani, 2001). Hjuler and Fabricius (2009) describe the chalk as having clear signs of recrystallization, contact cements, overgrowth, and particle interlocking but preserved intrafossil porosity and with commonly

well-preserved coccolithophores. Beside calcite, noncarbonate phases (ca. 5 wt.%) are represented by quartz, smectite, mica, and clinoptilolite and traces of apatite, feldspar, pyrite, and titanium oxides. After deposition, the Liège chalk only slightly suffered from early diagenetic cementation (Hjuler and Fabricius, 2009), as pelagic limestones are composed mostly of low-Mg calcite and are not prone to this process (Molenaarand Zijlstra, 1997). The Liège chalk was only subjected to shallow burial and still contains approximately 40%-45% primary porosity (Hjuler and Fabricus, 2009).

EXPERIMENTAL PROCEDURES

Sampling

Large sample blocks were taken from the quarry close to Hallembaye (CBR-Lixhe [Cimenterie Belge Reunié] quarry; Slimani, 2001) in the region of Liège (Belgium) at N50°44 ′51.16″ and E005°38′52.17″. The chalk was studied earlier in detail regarding its petrology and mineralogical and rheological characteristics (Felder, 1975; Molenaar and Zijlstra, 1997; Slimani, 2001; Strand et al., 2007; Hjuler and Fabricius, 2009). The samples were broken out as large blocks of 0.5–1 m^3 and then sampled directly from cleaned fresh surfaces. The sample was cored from the chalk block assuring minimum contamination of the sample, and was shaped into a cylinder with a diameter of 38 mm and cut to a length of 70 mm (Figure 1). After shaping, the core was dried for 24 hr at 130°C in a drying furnace and weighed before it was saturated with distilled water in a vacuum vessel. The pore volume (PV) was obtained by the weight difference between the saturated and dry core sample, and the porosity was estimated from the ratio of the PV divided by the bulk volume of the sample (40.5%).

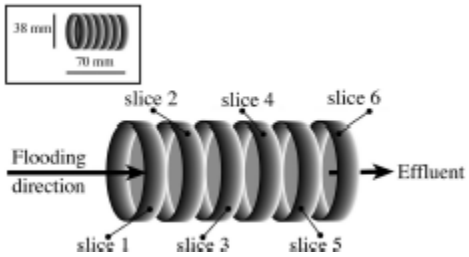

Figure 1. Sketch of experimental set-up for the long-term test. MgCl2fluid was injected from the left into the sample core and the effluent collected on the right. The core (ca. 7 cm long) was cut into six slices with thicknesses of about 1 cm (illustrated as separated units). The diameter of 3.8 cm allows for probing the sample with different methods.

Mechanical Flow Through Experiment

The chalk core was mounted in a standard hydraulically operated triaxial cell and cleaned by flooding two initial PVs of distilled water to insure a clean pore system. The confining (isotropic) pressure and pore pressure were simultaneously increased from 0.5 and 0 MPa to 1.2 and 0.7 MPa, with a constant stress difference (i.e. effective stress given that the Biot coefficient is 1) of 0.5 MPa. The cell was equipped with a heat-regulating system that kept the temperature constant at 130 ± 0.1°C during the experiment. The axial displacement was measured by an outside linear voltage displacement transducer (±0.01 mm), which follows the movement of the piston. After the sample was cleaned by distilled water we injected 0.219 M $MgCl_2$ brine at a constant injection rate of 32.4 ml/day (i.e., 1 initial PVs/day). This injection rate was constant throughout the experimental program, leading to a total of 16.4 L injected. Then, the hydrostatic stress was increased from 1.2 to 12.6 MPa over 320 min. In this hydrostatic loading phase, the stress-strain curve enabled us to estimate the elastic and yield parameter of the sample. After the loading phase, the pore and hydrostatic stress was constant for 516 days, although we monitored the axial strain development during continuous flooding of $MgCl_2$ brine.

To study changes in the ionic composition of the injected brine, the effluent was sampled three times a week throughout the creep phase (516 days). After the experiment, the brine was displaced by distilled water to avoid salt precipitation and the dried core cut into six slices with thicknesses of about 1 cm for subsequent analyses of the core material.

Chemical Analyses of the Effluent

The ionic concentrations were analyzed with a Dionex ICS-3000 ion-exchange chromatograph. The analyses were performed with ICS-3000 conductivity detector. IonPac AS16 and IonPac CS12A were used as anion and cation exchange columns, respectively. The sampled effluents were diluted to stay in the linear region of the calibration curve, and ionic concentrations were calculated based on an external standard method.

Scanning Electron Microscopy

Surfaces of freshly broken core chips were imaged using a Zeiss Supra 35VP field emission scanning electron microscopy (SEM) in high vacuum mode with an accelerating voltage of 12 kV, aperture size of 30 μm, and working distance of 10–12 mm. EDAX Genesis energy-dispersive x-ray spectroscopy (EDS) was applied for determining the semiquantitative elemental and mineralogical composition of the samples. The EDS measurements were acquired together with the corresponding SEM microscopic images. Because the core dominantly consisted of calcite, the EDS system was calibrated against an Iceland spar calcite crystal. Both flooded and unflooded samples are analyzed. The unflooded samples are the end pieces of the sample and are from the same piece of chalk.

X-ray Diffraction

Samples in random mounts were analyzed on a Philips X'Pert PRO PW 3040/60 diffractometer, with Cu Kα x-ray radiation, Si monochromator, at 40 kV and 30 mA. Step scan at ~1.5°/min and step size of 0.02° 2θ.

Whole-Rock Geochemistry

Samples were carefully separated from the main core and milled to a fine mesh in an ultraclean agate mill. Geochemical data for all major and trace elements were obtained using inductive coupled plasma mass spectrometry analysis at Acme laboratory (Vancouver, Canada). Detection limits and detailed description of the analytical process and certificates can be downloaded from http://acmelab.com. Other information is included in Table 1.

Nano Secondary Ion Mass Spectrometry (Nano-SIMS)

Sample fragments of approximately 1 cm^3 were prepared for nano secondary ion mass spectrometry (nano-SIMS) analyses by polishing and mounting in epoxy-blocks in a one-inch-diameter ring. The analyses were performed on the NanoSIMS 50 instrument (CAMECA, Gennevilliers, France). The surface of the sample was scanned with a focused 8 kV Cs+ primary beam. The current was in the range of 1–2 pA, which results in a beam expected to be smaller than 100 nm in diameter (lateral resolution). The images had a spatial size of 5 × 5 to 40 × 40 μm^2 and the image size 256 × 256 pixels, leading to a pixel resolution from20 to 160 nm per pixel. The secondary beam, induced by the primary impact, was collected with a secondary acceleration of −8 kV. Once the ions were filtered in energy and in mass according to the ratio *m/z*, they were recorded in the multicollection system of the NanoSIMS 50. The masses detected were ^{12}C, ^{16}O, ^{35}Cl, ^{28}Si, $^{24}Mg^{16}O$, and $^{40}Ca^{16}O$.

Table 1. (A) Selected Geochemical Data of the Long-Term Test Samples Compared to the Data from 5 Samples of the Same Exposure in the Belgium Chalk*; (B) Normalization of the Geochemical Composition of the Altered Slices Versus LT; (C) Geochemical Variation in Percent, in Altered Slices Versus LT†

Sample	Unit	SiO_2 %	Al_2O_3 %	MgO %	CaO %	Sr ppm	TOT/C %	Rb ppm	Zr ppm	Y ppm
(A)										
LT1	First slice	4.68	0.89	33.03	14.43	244.2	12.53	3.7	18.0	8.7
LT3	Third slice	4.05	0.68	6.99	45.58	815.6	11.61	2.7	15.6	8.3
LT4	Fourth slice	3.94	0.71	3.88	49.42	876.0	11.47	2.9	14.9	6.9
LT5	Fifth slice	3.93	0.71	3.18	49.87	1019.1	11.48	2.8	14.0	8.4
LT6	Sixth slice	4.22	0.73	3.03	50.15	1015.6	11.55	3.0	13.9	8.9
LT7	Not tested inlet	4.37	0.70	0.33	52.22	1096.2	11.66	6.2	15.7	7.8
LT8	Not tested outlet	4.99	0.73	0.39	51.82	1089.2	11.66	6.3	15.5	7.3
LT†		4.68	0.72	0.36	52.02	1092.7	11.66	6.3	15.6	7.55
(B)										
LT1/LT	First slice	1.00	1.24	91.75	0.28	0.22	1.07	0.62	1.15	0.56
LT3/LT	Third slice	0.86	0.94	19.42	0.88	0.75	0.99	0.45	1.00	1.00
LT4/LT	Fourth slice	0.84	0.99	10.78	0.95	0.80	0.98	0.48	0.96	0.96
LT5/LT	Fifth slice	0.84	0.99	8.83	0.96	0.93	0.98	0.47	0.90	0.90
LT6/LT	Sixth slice	0.90	1.01	8.42	0.96	0.93	0.99	0.50	0.89	0.89
(C)										
LT1/LT	First slice	0	24	9075	−72	−78	7	−38	15	−44
LT3/LT	Third slice	−14	−6	1842	−12	−25	−1	−55	0	0
LT4/LT	Fourth slice	−16	−1	978	−5	−20	−2	−52	−4	−4
LT5/LT	Fifth slice	−16	−1	783	−4	−7	−2	−53	−10	−10
LT6/LT	Sixth slice	−10	1	742	−4	−7	−1	−50	−11	−11

*See Table S1 for the complete data set, supplementary material available as AAPG Datashare 61 at www.aapg.org/datashare.
†LT is the value calculated as average of the untested samples LT7 and LT8; % = weight percent; ppm = parts per million; TOT/C = total carbon.

RESULTS

Characteristics of Unflooded Chalk from Liège

The unflooded samples, i.e., the end pieces acquired from the cutting of the chalk core before mounting the triaxial cell, are called L7 and L8. The x-ray diffraction (XRD) combined with field emission-scanning electron microscopy (FE-SEM) and whole-rock geochemistry reveal that the sample has a carbonate content of 94.7 wt.% (Figure 2, T able 1, Table S1 in supplementary material available as AAPG Datashare 61 at www.aapg.org/datashare). This is comparable to Hjuler and Fabricius (2009), who report approximately 98 wt.% for Liège chalk. Observed slight variations in the composition are expected for different samples from the same exposure. Other less abundant minerals are quartz, mica, illite, and kaolinite, with significantly lesser amounts of opal-CT (opal-cristobalite-tridimite), zeolite, feld-spar, siderite , sylvite, and pyrite resulting from SEM and X RD studies. Most of the calcite derives from dispersed or intact coccoliths (Figure 2). The EDS analyses illustrate the calcite dominated mineralogy, whereas O, Ca, and C are the most abundant elements. Si accounts for only about 1.5–2.5 wt.%, whereas Al, Mg, and K occur in amounts of generally less than 0.5 wt.%.

The geochemical analyses from the whole-rock geochemistry of the untested chalk (samples LT7 and LT8, Table 1, Table S1 in supplementary material available as AAPG Datashare 61 at www.aapg.org/datashare) show a relatively small amount of noncarbonate phases with concentrations of SiO_2 between 4.37 and 4.99 wt.%, Al_2O_3 between 0.70 and 0.73wt.%, MgO between 0.33 and 0.39 wt.%, extremely low Fe_2O_3 concentrations (ca. 0.32–0.37 wt.%) and CaO at approximately 52 wt.%. Besides using minor elements such as Al_2O_3, clastic input can be identified with high trace element concentrations of Rb (c a. 6 ppm), Y (7–8 ppm), and Zr (ca. 15–16 ppm) (e.g., Frimmel, 2009). These values are in the range of 5%–10% of typical upper continental crust (McLennan e t al., 2006) and indicate significant clastic input for a carbonate rock (Frimmel, 2009). Rare earth element (REE) patterns do not entirely reflect typical seawater composition, as middle REEs are slightly enriched, but show characteristic Ce⁄Ce*,Eu⁄Eu*,and La⁄La* anomalies (Table S1 in supplementary material available as AAPG Datashare 61 at www.aapg.org/datashare; Nozaki et al., 1997; Frimmel, 2009). Y/Ho ratios with 37 and 33 for LT7 and LT8, respectively, point to the influence of a secondary fluid

percolating in the chalk (Nozaki et al., 1997). These values are typical for Liège chalk and the ratio remains unaffected by fluid injection during the presented long-term experiment (Table S1 in supplementary material available as AAPG Datashare 61 at www.aapg.org/datashare).

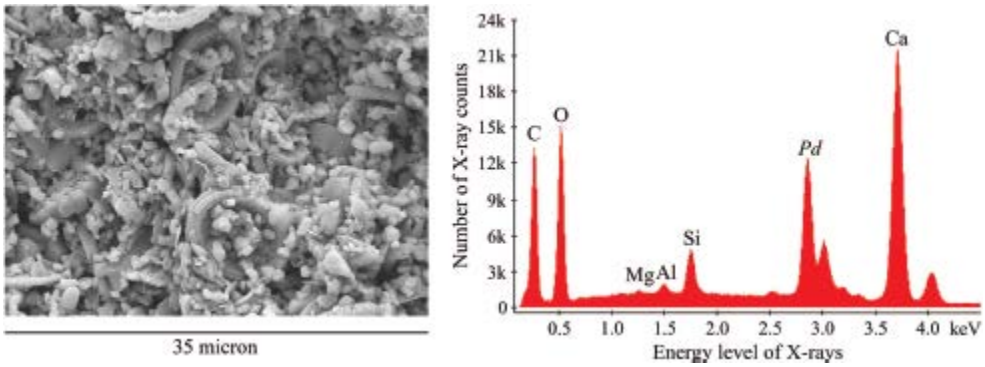

Figure 2. Unflooded core material. Scanning electron microscopy micrograph and associated energy-dispersive x-ray spectroscopy spectrum of the image area's bulk elemental composition dominated by Ca, C, and O; the sample was sputter coated with palladium (Pd). The chalk material consists mainly of intact or dispersed coccoliths composed of calcite.

Experimental Findings

Compaction and Chemical Analyses of Fractioned Effluent

The chemical analyses of the effluent fluid samples show that during the entire injection period, the Cl^- concentration remains close to its original concentration (Figures S2, S3 in supplementary material available as AAPG Datashare 61 at www.aapg.org/datashare). In addition, the $Ca2^+$ concentration in the effluent fluid has been increased, whereas a significant loss of Mg^{2+} is observed. On average, the Mg^{2+} and Ca^{2+} concentrations stay constant around0.195 and 0.022 mol/L, respectively with a total Mg^{2+} + Ca^{2+} concentration of 0.217 mol/L. This is close to the original magnesium concentration of the injected brine (0.219 M $MgCl_2$) indicating that the Mg-Ca exchange is the most important player in the stoichiometric calculations of the rock-fluid interactions. The fact that the sum of Mg^{2+} and Ca^{2+} concentration and the injected Mg^{2+}-concentration deviate opens up the possibility that other cations are produced from the core (see Figures S2, S3 in supplementary material available as AAPG Datashare 61 at www.aapg.org/datashare).

Based on the geochemical methods, the amount of dissolved calcite from the rock matrix is considerable, as the total Ca^{2+} production from the rock is approximately 13.5 g, meaning that as much as 20% of the core had been dissolved during the experiment. Strain measurements demonstrate that after 516 days of creep, the core experienced axial shortening of 18% to a length of 57.65 mm. Because the pore and bulk volume changes in this drained mechanical experiment related through the Biot coefficient, we estimate the porosity changes from bulk strain measurements alone by making an appropriate value of 0.8 for the Biot coefficient (Fjær et al., 2008; Omdal et al., 2009). The evolution of porosity with time is illustrated in Figure S2 (supplementary material available as AAPG Datashare61 at www.aapg.org/datashare). The final porosity of the core is calculated to be 31.5%, which corresponds to a relative reduction of approximately 20% compared to its original value (40.5%).

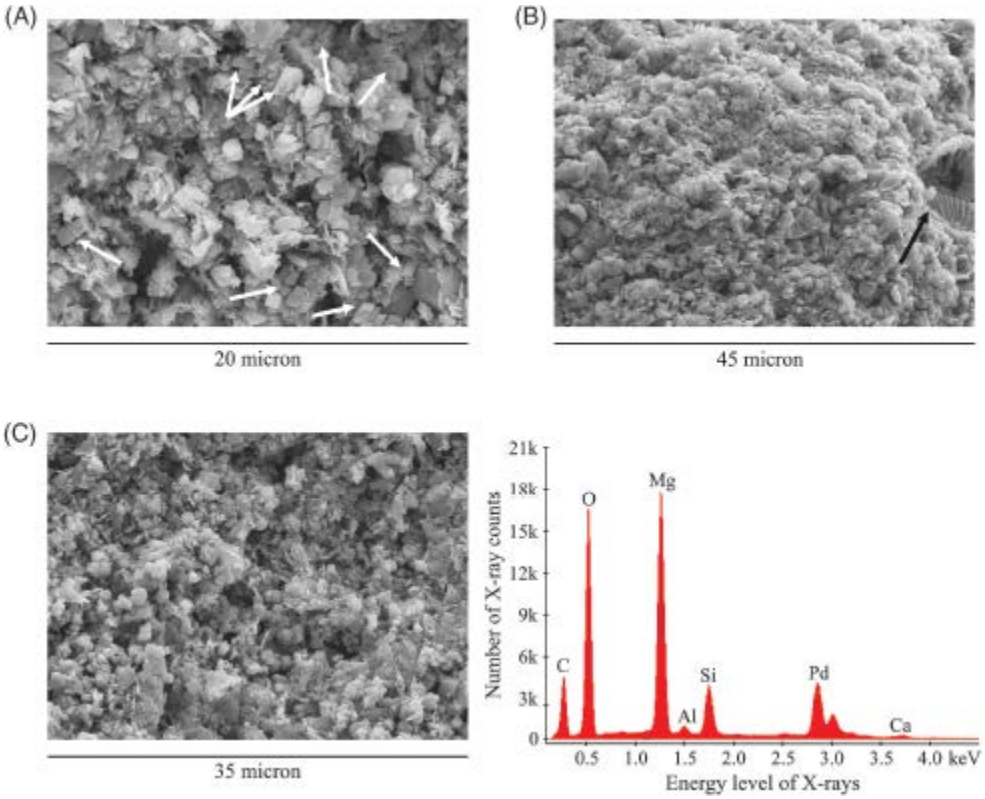

Figure 3. Flooded core material. (A) Scanning electron microscopy (SEM) micrograph shows common occurrence of magnesite crystals with rhombic habit (arrows) and absence of coccolith remains. (B) SEM micrograph illustrates badly preserved calcite matrix with signs of dissolution and loss of porosity; arrow points to preserved coccosphere. (C) SEM micrograph and associated energy-dispersive x-ray spectroscopy spectrum of the image area's bulk elemental composition dominated by Mg, C, and O; the sample was sputter coated with palladium (Pd).

Chalk Characteristics After the Experiment

After flooding with $MgCl_2$ brine, the mineralogical morphology of the Liège chalk appears severely altered in the first two slices (LT1 and LT2). The SEM images in Figure 3A, B, and C illustrate variation in the observed changes in texture and composition after flooding. In Figure 3A, the occurrence of angular well-formed rhombic magnesite grains are shown with arrows. The coccoliths that were frequently seen in the unflooded chalk samples (LT7 and 8) can now only rarely be found. In Figure 3A, no coccolith remains can be seen, but one is still preserved in Figure 3B.The preserved calcitic material shows grain rounding and loss of angularity, which is a clear sign of severe dissolution. In short, dissolution of calcium-containing minerals can be observed, whereas magnesium-bearing minerals are observed in higher abundances. This is supported by the semiquantitative EDS spectrum of the same SEM micrograph in Figure 3C. Here, the chemical change is recognized by the high abundance of O, Mg, and C, and the Si amount is approximately doubled, whereas at the same time Ca accounts for only less than 1.5 wt.%.

Figure 4 displays the results of XRD analyses of the flooded core within slices LT1 to LT6, and the unflooded end pieces LT7 and LT8. The XRD measurements show some silicate minerals (quartz and anthophyllite), as well as gypsum and calcite (Figure 4). The only other carbonate phase is magnesite as well as traces of another magnesium-bearing mineral, such as chrysotile formed from the interaction of quartz and $MgCl_2$. Magnesite abundancy is largest at the inlet slice LT1 and decreases in abundance along the core. Magnesite can be traced up to the third slice LT3. In LT4, magnesite could not be detected anymore. Interestingly, scarce amounts of tilleyite ($Ca_5Si_2O_7(CO_3)_2$) appear in LT4, which is

not observed in the other samples (Figure 4). The LT5 and LT6 samples display a spectrum dominated by calcite, a signal very similar to the unflooded cores LT7 and LT8 except one very important observation: All the quartz and gypsum that is observed in the unflooded samples is dissolved. The dissolution of quartz is observed for all flooded samples. In Madland et al. (2013), dolomite could only be detected at the rim of LT1 as intrafossil filling of foraminifera shells. Here, no dolomite is observed (Figure 4), and we believe that this might be because the amount of dolomite is below the detection limit of the XRD.

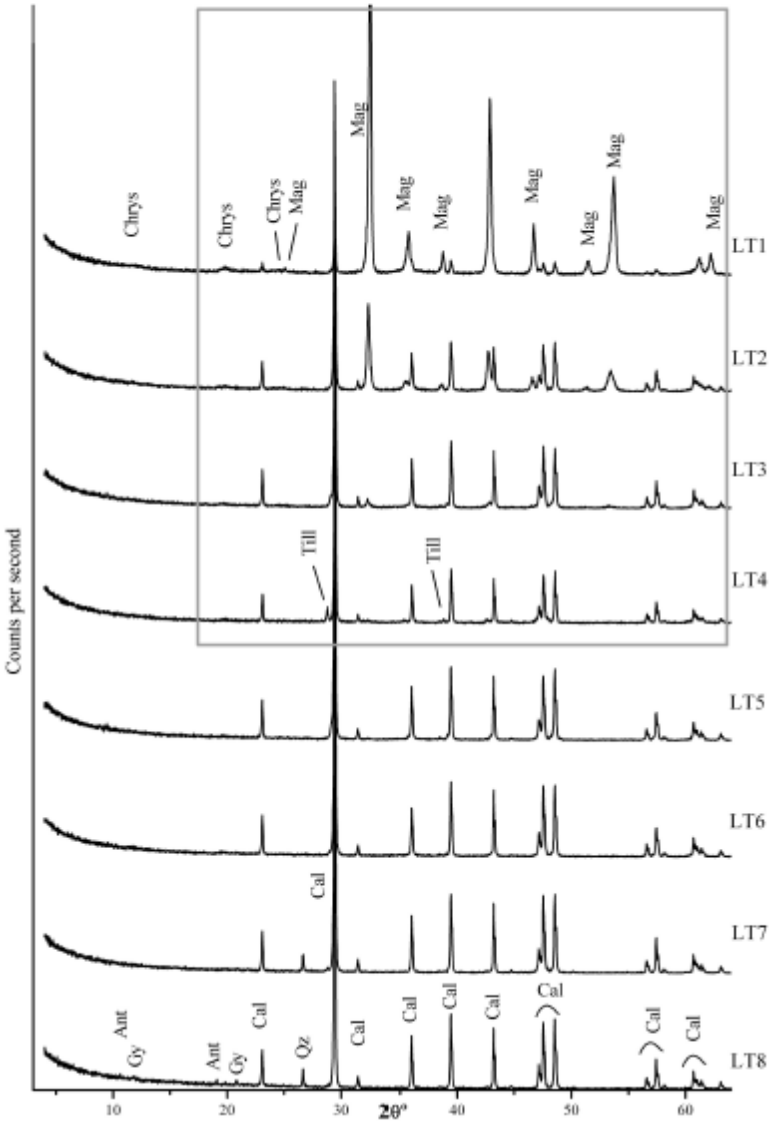

Figure 4. X-ray diffraction mineralogy of the flooded slices of the core (LT 1–6) and unflooded chalk (LT 7 and LT 8) from Liège. Cal = calcite; Mag = magnesite; Qz =quartz; Ant = anthophyllite; Gy = gypsum; Till = tilleyite; Chrys =chrysotile. Gray rectangle marks the range where most significant changes are observed from slice LT1 to LT4.

In Table 1A, the concentrations of selected major and trace elements are presented from the whole-rock geochemistry. The data show where the chemical alteration occurs downstream the sample from slices LT1 to LT6. The silica concentrations show slight reduction from LT3 to LT6, with the highest value for LT1 similar to the concentration found in the unflooded chalk (Table 1A, B). Small changes can be observed in the total carbon (TOT/C) concentration, which is the highest in slice LT1, higher

than in the untested sample and in all other slices. Significant differences could not be observed for Na_2O and K_2O, although the concentrations do change slightly (see Table S1 in supplementary material available as AAPG Datashare 61 at www.aapg.org/datashare). The most significant changes are observed for CaO and MgO. The MgO concentration in slice LT1 is enriched by 91 times the original value, from 0.36 to 33.03 wt.%. The same spatial pattern as described earlier is seen in this analysis where the chemical alteration is reduced downstream. In slice 3, the MgO concentration is 20 times the original value. In slices 4, 5, and 6, the MgO concentration is increased by a factor 10, 8, and 7, respectively (see Table 1, Figure S1 in supplementary material available as AAPG Datashare 61 at www.aapg. org/datashare). Although being semiquantitative, we may still explore the spatial variation of chemical alteration downstream the sample with the EDS measurements. The increase in MgO concentration downstream the sample attains the values 106, 81, 12, 10, and 8, and eight times the original concentration from slices LT1 to LT6.

As indicated by the effluent data, stoichiometry is almost conserved in the effluent by considering the ion exchange between calcium and magnesium. The same relation between Mg^{2+} and Ca^{2+} is reflected in the mineralogical observations. The whole-rock geochemistry shows that the CaO concentration decreases by 72% in slice LT1, from 52 wt.% on unflooded Liège chalk to 14wt.%. The same spatial pattern is observed in flooding direction as the observed chemical alteration is reduced to 12%in slice LT3, and 5%, 4%, and 4% in slices 3 to 6, respectively (Table 1, Figure S1 in supplementary material available as AAPG Datashare 61 at www.aapg.org/datashare). The EDS measurements show a similar decreasing trend as the whole-rock geochemistry with the values 97, 81, 11, 9, and 8, and 8% from LT1 to LT6. The same trend can be observed in Sr concentrations (Figure S1 in supplementary material available as AAPG Datashare 61at www.aapg.org/datashare). The Sr can replace Cain carbonate or other Ca-bearing minerals like plagioclase or apatite. These geochemical data suggest that more than 50% of slice LT1 changed entirely in terms of mineralogy after injection of the fluid, which supports the results from the SEM and XRD datasets.

The SEM-EDS results showed precipitation of magnesite in slice LT1, but the mineral was also detected at much lower abundances in all slices. Concentration increased by approximately 100 times in the first slice, down to only 7–10 times in slices LT4 to LT6 (Table 1).

To constrain the detailed chemical alteration at sub-grain scales, we used NanoSIMS 50 (Krein et al., 2008). Figure 5A shows the element map across 5 ×5 μ sized image of slice 1. The grayscale indicates the number of electron counts. Three elements are shown, namely silicon, magnesium, and calcium. Figure 5A shows the proof of the proposed mineralogical growth of magnesite in slice 1 (Figure 5A), which also occurred in slice 4 (not shown here), because magnesite does not occur in unflooded Liège chalk (Figure 4). It can be observed in Figure 5A that the center of the yellow polygon is completely lacking CaO (see values in Figure 5A), whereas other areas hold significant abundances of CaO (lighter grayscales). The composition of the marked area (Figure 5A) is dominated by ions of MgO. The abundance of carbon can be explained by a high sensitivity of the SIMS technique for the analysis of the carbon (Valle et al., 2006). Also, Figure 5A shows quartz crystals of 1 –2 μm in the chalk (marked by the stippled red line; left image). In Figure 5B, acquired from L1, a wide dissemination of clay-sized quartz in the chalk together with abundant MgO can be observed. Both phases, silica and magnesium, seem to be present in the entire rock as a result of the introduction of $MgCl_2$ brine leading to subsequent dissolution and precipitation.

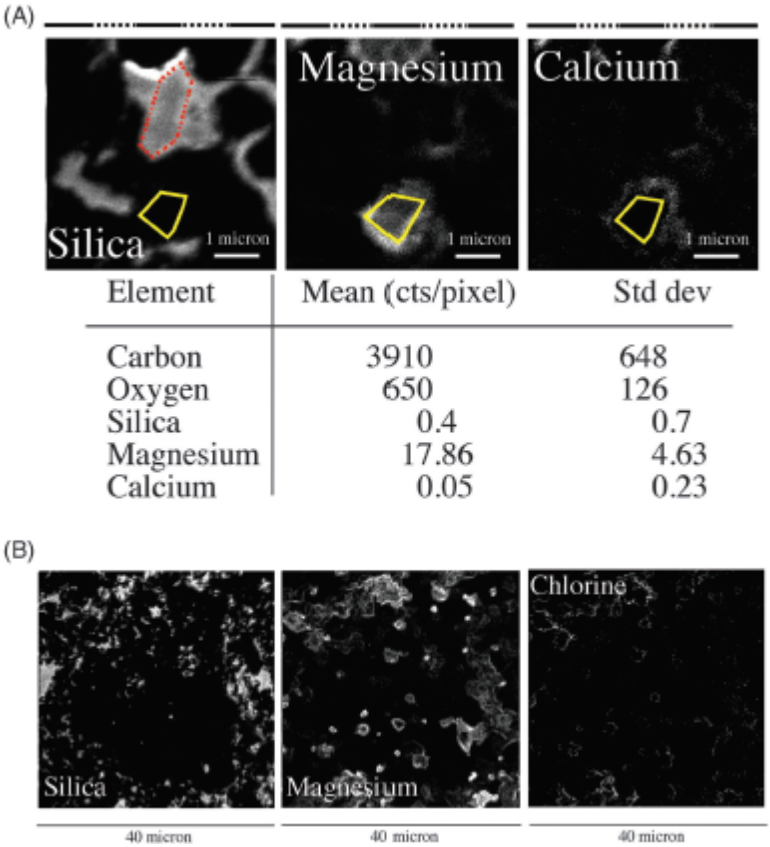

Figure 5. (A) Nano-SIMS (secondary ion mass spectrometry) picture of an area measuring 5 µ in slice 1. One micron scale bar is shown on top of the three selected ions (^{28}Si, ^{40}Ca, ^{25}Mg) as stippled and black lines. Every scan is 5 × 5 µm with 256 pixels resulting in a pixel size of approximately 20 nm. Magnesite is shown within the light-colored box at the bottom center of the picture. The table in the figure shows the detection of the different ion abundances (counts per pixel; see section "Experimental Procedures") and demonstrates the absence of CaO in the yellow marked area (ca. 0.8 µm^2). ^{12}C and ^{16}O are easy to ionize and abundant, therefore, not shown here. The table demonstrates the absence of CaO in the new grown mineral. (B) Nano-SIMS picture of an area measuring 40 µm (pixel size ca. 150 nm). Shown are the abundances of ^{28}Si (left), ^{25}Mg (center), and Cl (right) ions in slice 1. The gray scales of abundances cannot quantify the amount, but identify the intensity in relation to ion target. Cts = counts; Std. dev. = standard deviation.

Evaluation of the compositional changes during flooding of reactive fluids using scanning electron microscopy, nano-secondary ion mass spectrometry, x-ray diffraction and whole rock geochemistry

By using the lattice Boltzmann geochemical model (Hiorth et al., 2013), it is possible to predict the effluent curve in this experiment (Figure S3 in supplementary material available as AAPG Datashare 61 at www.aapg.org/datashare) and at the same time, where in the core the chemical alteration occurs. The model reflects a sharp alteration front where the first part is nearly completely altered from calcite to magnesite. In Table S2A (supplementary material available as AAPG Datashare 61 at www.aapg.org/datashare), the assumed mineralogical change per PV flooded is shown, where quartz in the core is expected as being converted to talc, and magnesite is produced. Although the geochemical model predicts that the talc should be precipitated, we were not able to detect this with the tools presented here. This could be because the concentration is too low for the XRD to detect it, nano-SIMS studies cover only a very small field of view, and because the degree of heterogeneity is so large it cannot be used for whole-rock studies. At the same time, the FE-SEM-EDS analysis has too large a spot size to identify talc grains of size less than 1–2 µ beyond doubt.

IMPLICATION OF THE EXPERIMENTALRESULTS

The injection of $MgCl_2$ for 516 days under Ekofisk reservoir stresses and 130°C produced significant compositional changes in the Liège chalk (Belgium). In the first 2 cm of the sample, large amounts of magnesite had grown and much of the calcite was dissolved (Figures 2, 3). Geochemical analyses of the different slices affected by fluid flow demonstrated massive enrichment of MgO and depletion of CaO in the tested core (Table 1, Table S1 in supplementary material avail-able as AAPG Datashare 61 at www.aapg.org/datashare). Additionally, we suspect that other Mg-bearing minerals, one of which we identified as chrysotile with XRD, might have precipitated together with very little amounts of Fe, Si, and Al based on SEM-EDS analyses. Geochemically, no other major element showed significant variation in its concentration. The increase of silica in LT1 is nearly negligible, and the loss in LT3 to LT6 is in the order of 10–15 wt.%. The XRD showed that no quartz could be detected in the flooded samples (LT1 to LT6), although the whole-rock geochemistry showed a variation from 4.68 to 4.22 wt. %. This indicates that other non quartz silicate phases are present in the core (Figure 5B). The whole-rock geo-chemistry, together with SEM-EDS data and nano-SIMS studies, clearly detects the decreasing trend of magnesite precipitation from the inlet along the core toward the outlet (Table 1, Figure 5). The new growth of magnesite is accompanied by the depletion of Sr similar to Ca. Sr could therefore in a future study represent a more sensitive marker of mineralogical changes than CaO.

The experimental results presented in this paper do not directly translate to a larger scale because in the field the injected water is colder than the reservoir. In the presented experiments, the injected water is heated on its way into the triaxial cell, whereas in a reservoir setting the injected cold water will cool the rocks close to the injector well. The kinetic rates of the geochemical reactions, together with the stable mineral phases during rock-fluid interactions, are temperature-dependent parameters. Typically, the kinetic rates are slower for lower temperatures. As such, an accurate temperature model and flow model are needed to understand how the presented geochemical alteration is transferred to the field scale. As the injected water is transported through the reservoir it gets heated, leading to a spread in the alteration front into the reservoir before equilibrium is attained at the rock-fluid interface. Although the alteration front will not be localized in the reservoir, it will still lead to chemically induced compaction. The additional compaction, which in part is a consequence of load-bearing structures dissolving, and in part because magnesite is denser than calcite, will change the solid volumes and therefore also the wettability, which will have a direct consequence for the recovery of hydrocarbons. However, it might also have an additional effect on the wetting properties of the sur-face, as the new mineral being formed most likely has a different surface energy than the primary mineral. However, this could be an interesting field for study in the future. Magnesite formation in the core during water imbibition and oil expulsion could be a possible explanation for the observations by Austad and Standnes (2003) (see also in Hiorth et al., 2010), where they find that magnesium in the invading brine increases the recovery of oil in an experiment with less than 1 PV, much less than the 516 PV we used in our experiment.

CONCLUSIONS

Injection of $MgCl_2$ into a Campanian chalk sample from Liège (Belgium) induced significant mineralogical changes. The experiment is unique because the brine was injected over an unusually long time (516 days) at 130°C and in situ effective stresses most of the flooding tests for EOR studies are far shorter. The chalk sample was sliced into six equal parts perpendicular to its long axis (Figure 1) and studied with SEM-EDS, whole-rock geo chemistry, XRD and nano-SIMS. The selected chalk contains not more than few percent of noncarbonate phases and is dominated by calcite (Figure 2, Table 1).

Our results show that:

• A new mineral phase grew in the first centimeters of the tested core (LT1), which is characterized by an increase of MgO about 90 times the original concentration and a depletion of CaO by more than 70% by weight (Table 1) . Other enrichments or depletions of elements were not observed, except for Sr, which is depleted in slices LT1 to LT4. The replacement of Ca by Mg decreases from slice LT1 toward the end of the sample, the core's outlet (Table 1).

• The new mineral phase, which grew in the tested core is dominantly magnesite, which precipitates as nano-sized rhombic crystals (Figure 3A). In slice 1 (Figure 1), magnesite is probably as abundant as 60%, or even more. The XRD-analysis showed that all the quartz has been removed from the core.

• Chlorine and silica disseminate as very small-grained phases in the chalk matrix commonly smaller than 1 μ), the latter even in the form of euhedral crystals (Figure 5A, B).

• At constant effective stress, the core significantly compacted, the porosity was reduced by 20%, and calcite was significantly leached out of the core (Figure S2 in supplementary material available as AAPG Datashare 61 atwww.aapg.org/datashare).

• Despite being classified as semiquantitative, the FE-SEM-EDS measurements provide the same trends as the whole-rock geochemistry in the quantification of the mineral assemblage after flooding. These results are important for various reasons. The injection of $MgCl_2$ brine alters nearly the entire mineral assemblage of the core in a geologically very short time (although it would take significant time to flood 516 PV in a natural setting). Rock properties such as mineralogy, geochemistry, and porosity are strongly affected. Understanding the mineralogical and chemical changes induced by brine injection is very important for EOR because (1) dissolution of chalk causes enhanced compaction. On one side, compaction represents an important mechanism to drive hydrocarbons toward production facilities, but on the other side it may be detrimental to the permeability of the flooded reservoir leading to water divergence leaving vast amounts of hydrocarbons behind, and (2) the formation of secondary minerals affects the rock surface properties and it may alter the flow pathways for oil and water. The observed textural changes in the chalk allow different fluid flow mechanisms to play a role in reservoirs. This knowledge offers a wide range of further research to search for more optimal production strategies to enhance the oil production from chalk reservoirs. A large field of further research could examine whether magnesite is the sole product of this mineralogical change or whether other phase changes occur earlier and are of significant importance for EOR processes.

ACKNOWLEDGEMENTS

We would like to thank V. Morosova for the preparation of untreated chalk samples for geochemistry and C-O isotope measurements. The authors thank BP Norge AS and the Valhall coventurers, including Hess Norge AS, as well as ConocoPhillips and the Ekofisk coventurers, including Total E&P Norge AS, ENI Norge AS, Statoil Petroleum AS and Petoro AS for financial support. The research program Women in Natural Sciences by UiS is also thanked for financial support. We thank the editor S. E. Laubach for his comments and editorial efforts, and the two reviewers of the manuscript for their thoughtful and positive comments, as well as F. Whitehurst for her beneficial remarks.

DATASHARE XX

Figures S1, S2, S3, Tables S1, and S2 are available in an electronic version on the AAPG website

(www.aapg.org/datashare) as Datashare XX.

REFERENCES CITED

Austad, T., and D. C. Standnes, 2003, Wettability and oil recovery from carbonates: Effects of temperature and potential determining ions: Journal of Petroleum Science and Engineering, v. 39, no. 3–4, p. 363–376, doi:10.1016/S0920-4105(03)00075-5.

BP, 2014, Clair Ridge—Clair is located 75 km west of the Shetland Islands in 150 m of water and extends over an area of 220 km2, accessed M arch 2, 2015, www.bp.com/en/global/corporate/about-bp/bp-worldwide/bp-united-kingdom/bp-in-the-north-sea/clair-ridge.html.

Doornhof, D., T. G. Kristiansen, N. B. Nagel, P. D. Pattillo, and C. Sayers, 2007, Compaction and subsidence: Oil Field Review, v. 18, p. 50–68.

Fabricius, I. L., 2007, Chalk: Composition, diagenesis and physical properties: Bulletin of the Geological Society of Denmark, v. 55, p. 97–128.

Felder, W. M., 1975, Lithostratigrafie van het Boven-Krijt en het Dano-Montien in Zuid-Limburg en het aangrenz endegebied, in W. H. Zagwijn and C. J. van Staalduinen, eds., Toelichting bij Geologische overzichtskaarten van Nederland: Haarlem, Rijks Geologische Dienst, p. 63–72 (in German).

Fjær, E., R. M. Holt, P. Horsrud, A. M. Raaen, and R. Risnes,2008, Petroleum related rock mechanics, 2nd ed.: Oxford, Elsevier, 514 p.

Frimmel, H. E., 2009, Trace element distribution in Neoproterozoic carbonates as palaeoenvironmental indicator: Chemical Geology, v. 258, no. 3–4, p. 338–353, doi:10.1016/j.chemgeo.2008.10.033.

Hancock, J. M., 197 5, The petrology of the chalk: Proceedings of the Geological Association, v. 86, no. 4, p. 499–535, doi:10.1016/S0016-7878(75)80061-7.

Heggheim, T., M. V. Madland, R. Risnes, and T. Austad, 2005, A chemical induced enhanced weakening of chalk by seawater: Journal of Petroleum Science and Engineering, v. 46, no. 1–4, p. 11–18, doi:10.1016 /S0920-4105(00)00016-4.

Hellmann, R., P. J. N. Rrenders, J.-P. Gratier, and R. Guiguet, 2002, Experimental pressure solution compaction of chalkin aqueous solutions. Part 1. Deformation behavior and chemistry: The Geochemical Society, Special Publication, v. 7, p. 129–152.

Hermansen, H., G. H. Landa, J. E. Sylte, and L. K. Thomas, 2000, Experiences after 10 years of waterflooding the Ekofisk Field, Norway: Journal of Petroleum Science and Engineering, v. 26, no. 1–4, p. 11–18, doi:10.1016/S0920-4105(00)00016-4.

Hiorth, A., L. M. Cathles, and M. V. Madland, 2010, The impact of pore water chemistry on carbonate surface charge and oil wettability: Transport in Porous Media, v. 85, no. 1, p. 1-21, doi:10.1007/s11242-010-9543-6.

Hiorth, A., E. Jettestuen, L . M. Cathles, and M. V. Madland, 2013, Precipitation, dissolution, and ion exchange processes coupled with a lattice Boltzmann advection diffusion solver: Geochimica et Cosmochimica Acta, v. 104, p. 99–110,doi:10.1016/j.gca.2012.11.019.

Hjuler, M. L., 2007, Diagenesis of Upper Cretaceous onshore and offshore chalk from the North Sea area: Ph.D. thesis, Institute of Environment and Resources, Technical University of Denmark, Lyngby, 31 p., ISBN: 978-87-91855-42-9.

Hjuler, M. L., and I. Fabricius, 2009, Engineering properties of chalk related to diagenetic variations of Upper Cretaceous onshore and offshore chalk in the North Sea area: Journal of Petroleum Science and Engineering, v. 68, no. 3–4, p. 151–170, doi:10.1016/j.petrol.2009.06.005.

Korsnes, R. I., M. V. Madland, T. Austad, S. Haver, and G. Rosland, 2008a, The effects of temperature on the water weakening of chalk by seawater: Journal of Petroleum Science and Engineering, v. 60, no. 3–4, p. 183–193,doi:10.1016/j.petrol.2007.06.001.

Korsnes, R. I., S . Strand, Ø. Hoff, T. Pedersen, M. V. Madland, and T. Austad, 2006, Does the chemical interaction between seawater and chalk affect the mechanical properties of chalk?, in A. V. Cottheim, R. Charlier, J. F. Thimus, and J. P. Tshibangu, eds., Multiphysics coupling and long term behavior in rock mechanics: London, Taylor & Francis, p. 427–434.

Korsnes, R. I., E. Wersland, M. V. Madland, and T.Austad, 2008b, Anisotropy in chalk studied by rock mechanics : Journal of Petroleum Science and Engineering, v. 62, no. 1–2, p. 28–35, doi:10.1016/j.petrol.2008.06.004.

Krein, A., T. Udelhoven, J.-N. Audinot, C. Hissler, C. Guignard, L. Pfister, and H. N. Migeon, 2008, Imaging chemical patches on near-surface atmospheric dust particles with NanoSIMS 50 to identify material sources: Water, Air, and Soil Pollution: Focus, v. 8, no. 5, p. 495– 503, doi:10.1007/s11267-008-9182-x.

Madland, M. V., A. Finsnes, A. Alkafadgi, R. Risnes, and T. Austad, 2006, The influence of CO_2 gas and carbonate water on the mechanical stability of chalk: Journal of Petroleum Science and Engineering, v. 51, no. 3–4,p. 149–168, doi:10.1016/j.petrol.2006.01.002.

Madland, M. V., A. Hiorth, R. I. Korsnes, S. Evje, L. Cathles, T. Hildebrand-Habel, E . Omdal, and M. Megawati, 2011 Chemical alterations induced by rock-fluid interactions when injecting brines in high porosity chalks: Transport in Porous Media, v. 8 7, no. 3, p. 679–702, doi:10.1007/s11242-010-9708-3.

Madland, M. V., K. Midtgarden, R. Manafov, R. I. Korsnes, T. Kristiansen, and A. Hiorth, 2008, The effect of temperature and brine composition on the mechanical strength of Kansas chalk: International Symposium of the Society of Core Analysts, Abu Dhabi, UAE, October 29–November 2, 2008, 6 p.

Madland, M. V., U. Zimmermann, S. Haser, J.-N. Audinot,P. Gysan, R. I. Korsnes, B. Schulz, and A. Hiorth, 2013, Neoformed dolomite in flooded chalk for EOR processes: 75th EAGE Conference and Exhibition Incorporating SPE EUROPEC 2013, London, June 10–13,2013, 5 p.

McLennan, S. M., S. R. Taylor, and S. R. Hemming, 2006, Composition, differentiation, and evolution of continental crust: Constrains from sedimentary rocks and heat flow, in M. Brown and T. Rushmer, eds., Evolution and differentiation of the continental crust: Cambridge, Cambridge University Press, p. 92–134.

Molenaar, N., and J. J. P. Zijlstra, 1997, Differential early diagenetic low-Mg calcite cementation and rhythmic hard-ground development in Campanian–Maastrichtian chalk: Sedimentary Geology, v. 109, no. 3–4, p. 261–281, doi:10.1016/S0037-0738(96)00064-4.

Nagel, N. B., 2001, Compaction and subsidence issues within the petroleum industry: From Wilmington to Ekofisk and beyond: Physics and Chemistry of the Earth, Part A: Solid Earth and Geodesy, v. 26, no. 1–2, p. 3–14, doi:10.1016/S1464-1895(01)00015-1.

Nozaki, Y., J. Zhang, and H. Amakawa, 1997, The fractionation between Y and Ho in the marine environment: Earth and Planetary Science Letters, v. 148, no. 1–2, p. 329–340, doi:10.1016/S0012-821X(97)00034-4.

Omdal, E., R. Renli, T. G. Kristiansen, R. I. Korsnes, A. Hiorth,and M. V . Madland, 2009, Laboratory observations with implications for depletion of chalk reservoirs, in H. I. Ling, A. Smyth, and R. Betti, eds., Poromechanics IV: Proceedings of the 4th Biot Conference on Poromechanics: New York, DEStech Publication, p. 953–958.

Robaszynski, F., A. V. Dhondt, and J. W. M. Jagt, 2001, Cretaceous lithostratigraphic units (Belgium): Geologica Belgica, v. 4, p. 121–134.

Scholle, P. A., 1974, Diagenesis of Upper Cretaceous chalks from England, Northern Ireland, and the North Sea, in K. J. Hsüand H. C. Jenkyns, eds., Pelagic sediments: On land and under the sea: Boston, Blackwell Scientific Publications, p. 177–210.

Scholle, P. A., 1977, Chalk diagenesis and its relationship to petroleum exploration: Oil from chalks, a modern miracle?: AAPG Bulletin, v. 61, p. 982–1009.

Slimani, H., 2001, New species of dinoflagellate cysts from the Campanian-Danian chalks at Hallembaye and Turnhout (Belgium) and at Beutenaken (the Netherlands): Journal of Micropalaeontology, v. 20, no. 1, p. 1–11, doi:10.1144/jm.20.1.1.

Strand, S., M. L. Hjuler, R. Torsvik, J. I. Pedersen, M. V. Madland, and T. Austad, 2007, Wettability of chalk: Impact of silica, clay content, and mechanical properties: Petroleum Geosciences, v. 13, no. 1, p. 69–80, doi:10.1144/1354-079305-696.

Strand, S., D. C. Standnes, and T. Austad, 2003, Spontaneous imbibition of aqueous surfactant solutions into neutral to oil-wet carbonate cores: Effects of brine salinity and composition: Energy and Fuels, v. 17, no. 5, p. 1133–1144,doi:10.1021/ef030051s.

Taylor, S. R., and S. M. McLennan, 1985, The continental crust: Its composition and evolution: Oxford, Blackwell Scientific Publications, 312 p.

Thomas, L. K., T. N. Dixon, C. E. Evans, and M. E. Vienot,1987, Ekofisk waterflood pilot: Journal of Petroleum Technology, AIME Transaction, v. 283, p. 221–232.

Valle, N., J. Drillet, O. Bouaziz, and H. N. Migeon, 2006, Study of the carbon distribution in multi-phase steels using the NanoSIMS 50: Applied Surface Science, v. 252,no. 19, p. 7051–7053, doi:10.1016/j.apsusc.2006.02.283.

Zangiabadi, B., R. I. Korsnes, T. Hildebrand-Habel, A. Hiorth, I. K. Surtarjana, A. Lian, and M. V. Madland, 2009, Chemical water weakening of various out crop chalks at elevated temperature, in H. I. Ling, A. Smyth, and R. Betti, eds., Poromechanics IV: Proceedings of the 4th BiotConference on Poromechanics, DEStech Publication, p. 543–548.